

Acoustic Characterization of Resonance Wood

Marco Caniato, Stefano Favretto, Federica Bettarello, Chiara Schmid

University of Trieste, Department of Engineering and Architecture, Trieste, Italy. m.caniato@units.it

Summary

In this paper, a new approach for the characterization of resonance wood is described. In order to investigate how the wood microstructure influences final resonance performances, an intensive imaging analysis has been done, using innovative methods: X-ray synchrotron light micro-tomography coupled with the scanning electron microscopy. Several samples of *Picea Abies* (Spruce) from different provenances were tested in order to understand if their acoustic behavior is influenced by microstructure using a scientific approach. The geometrical and morphological information obtained by robust image processing analysis was used to feed a Finite Element Method model for further acoustic simulations. The method helped to show how the microstructure of this material determines its acoustical macro-behavior, allowing an objective sort between the high quality resonance wood and the worse one.

PACS no. 4335-c, 4335Mr

1. Introduction

In the last years several musicians, scientists and musical instruments makers/designers deal with the understanding of microscopic properties of different woods in order to realize, for example, piano soundboards.

At present, quality of resonance wood depends on subjective evaluation, which is not always accurate and efficient [1, 2]. The knowledge in this field is both from scientific approaches and from empirical methods or sometimes, as defined by Woodhouse [3] by “persistent folklore”. Many studies were carried out to determine the mechanical and micro-structural wood properties in order to link them to the resonance macro-behaviour and therefore to obtain measurable quantities [4, 5, 6]. Nowadays, for example, it is well known that spruce Young’s modulus for the violin front and back plate must be of a precise value [7]. Related to this topic, Bremaud in her complete works [8, 9] reported that “from an engineering sciences viewpoint, one can emit rather firm statements: “resonance wood” of spruce is naturally characterised by a very high axial E'/ρ and anisotropy, and low (but not extremely so) density and $\tan \delta$, where E' is the normalized Young’s modulus and ρ is the density”.

The relation between Young’s modulus and density is used [10, 11] to define the parameter called “radiation ratio” M as expressed by equation (1) and the relation between sound velocity and density is defined as “sound radiation coefficient” and is expressed by equation (2),

$$M = (E_1 E_2)^{1/4} / \rho^{3/2}, \quad (1)$$

$$R = c/\rho, \quad (2)$$

where E_1 and E_2 are the Young’s Moduli along and across the grain, ρ is the density and c is the material’s speed of sound.

There are nevertheless other parameters and variables which characterize and influence the resonance wood quality, such as the climatic conditions, moisture content [12], temperature fluctuations and type of drying.

The classification of different type of resonance wood is of paramount importance: diverse parameters may influence final instrument quality [13]. Rojas *et al.* [14] describe a simplified method capable of wood species identification using non-destructive technique (wave propagation). Several studies used ultrasound methods to understand mechanical properties [15, 16], while a few studies deal with modal analysis [17, 18, 19] or experimental measurements [20], concluding that only low frequencies are possible to be simulated, because middle-high frequencies take exponentially higher computational time. At the same deductions came other authors on other structures [21, 22] or different instruments [23]. FEM analysis was used by Bretos *et al.* [24] in order to determine mechanical properties and to simulate parameters variations. Boutillon and Ege [25] studied the influence of separated regime above and below a limit frequency using both modal and theoretical analysis. Wegst [26] reported the usual index related to the influence of density and the use of this parameter to choose the correct resonance wood for the desired musical instrument.

Moliński *et al.* [27] investigated the importance in the variations of mechanical properties within individual annual rings on resonance wood, while Spycher *et al.* [28] investigated physical and histological properties in order to assess resonance wood quality. Furthermore, Proto *et*

al. [29] deal with the opportunity to assess single standing trees resonance quality.

In her comprehensive study, Bucur [30] reports that it is generally admitted that generic term “resonance wood” (*Picea Abies*) is the first to be considered and that “the continuity and uniformity in the longitudinal direction of the anatomic structure play a more important role in the acoustic behaviour than its density”. From the Pearson and Webster studies [31] we can take for granted that the best piano soundboards are produced by European Spruce or Sitka one. Extensive studies for acoustical characterization on resonance wood are available [32, 33]; in these researches frequency methods on timber strips were used in order to determine Young’s modulus, sound velocity and internal frictions.

The aim of this paper is to evidence the importance of resonance wood microstructure as acoustic agent for the macro-behaviour of this material. A scientific method is then desirable in order to assess different resonance wood found in timber trade. This approach supplies a solid, objective and repeatable method to discriminate the various kind of wood in nature. This paper represents the conclusion of a previous research started by some authors [34, 35].

Non-invasive X-ray computed microtomography (μ -CT) was used combined with scanning electron microscopy (SEM) to image the inner wood structure.

In other studies [3, 30, 36], the microstructural behaviour is always linked to sound velocity, or density or mechanical properties like Young’s Modulus etc. These properties are tested in microscale but they do not depend on single cell geometry or disposition but on multiple cell distribution. As a matter of fact these properties (on microscale) could be thought as “macro-micro scale” since they are tested on wood strips, applying sensors to them. In this study, μ -CT, SEM and derived geometries were studied as a single micro-factor in order to understand if single cell geometry could influence macro acoustic behaviour. In a previous work, Kahle and Woodhouse [37] highlighted how the cells geometry could influence final elastic value.

Micro computed tomography (Figure 1) is one of the most advanced techniques in the field of non-destructive evaluation test. It allows internal microstructure imaging of different objects and materials, measuring the three-dimensional X-ray attenuation coefficient map of the investigated sample. X-rays pass through the object and the transmitted intensity is recorded as a two-dimensional image [38].

Radiation Intensity attenuation I is expressed by Beer-Lambert equation (3) under the assumption of a monochromatic X-ray beam,

$$I = I_0 \exp^{-\int_L \mu(\lambda) dx}, \quad (3)$$

where I_0 is the original intensity, I the final intensity, L is the length of the X-ray beam path and $\mu(\lambda)$ is the attenuation coefficient.

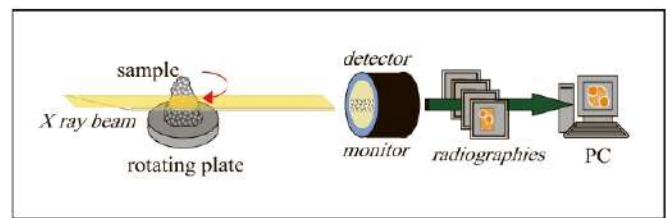


Figure 1. Micro computed tomography (μ -CT) scheme.

The acquired data are elaborated to calculate final results which consist of a sequence of bi-dimensional grayscale images, each one representing a horizontal slice of the original object. In other words, this means that tomography enables to look at slices of the investigated object without physically cutting it. When X-rays are produced by synchrotron light sources, a monochromatic parallel beam is formed, with a high brilliance and high spatial coherence, thus allowing both the traditional absorption scanning mode and the so called phase contrast tomography. The nominal resolution of a μ -CT dataset is usually given in terms of pixel size (or voxel size in 3D). In this case, the pixel size was of 45 micrometers.

2. Materials and methods

Samples provided by Fazioli Pianoforti (Italy) of three different quality of spruce (Spruce) and from different geographical sources (Figure 2) were analysed: (i) Val di Fiemme (Italy), (ii) Tarvisio Forest (Italy) and (iii) *Picea Sitchensis* (Canada); samples were chosen from different timber panels used to produce piano soundboards. The revealed micro-geometry was quantitatively investigated and further modelled in a finite element method (FEM) modal simulation comparing different microstructures.

Firstly, the quality sorting was performed by Fazioli Pianoforti (Italy) on the base of their long experience on resonance wood and according to literature [5]. The high quality Val Di Fiemme spruce was indicated by the piano producers as the best wood quality for musical instruments. This fact was taken for granted due to their long experience (about 50 years [30]) on high quality piano productions.

Five types of resonance wood (Table I and Figure 2) were analysed both with X-ray high resolution tomography (μ -CT) and Scanning electron microscopy. The obtained images were then used to build FEM microstructures models in order to understand the influence of different woods morphological compositions.

2.1. Investigation with X-ray μ -CT

X-ray high resolution tomography (μ -CT) was performed by synchrotron light at SYRMEP beam line of the ELETTRA synchrotron laboratory (Trieste, Italy). This technique is a powerful non-invasive technique for quantitative analysis of wood anatomical characteristics [39].

The light source, having a vertical size Σ (full width at half maximum - FWHM) of about 100 μ m, is produced by

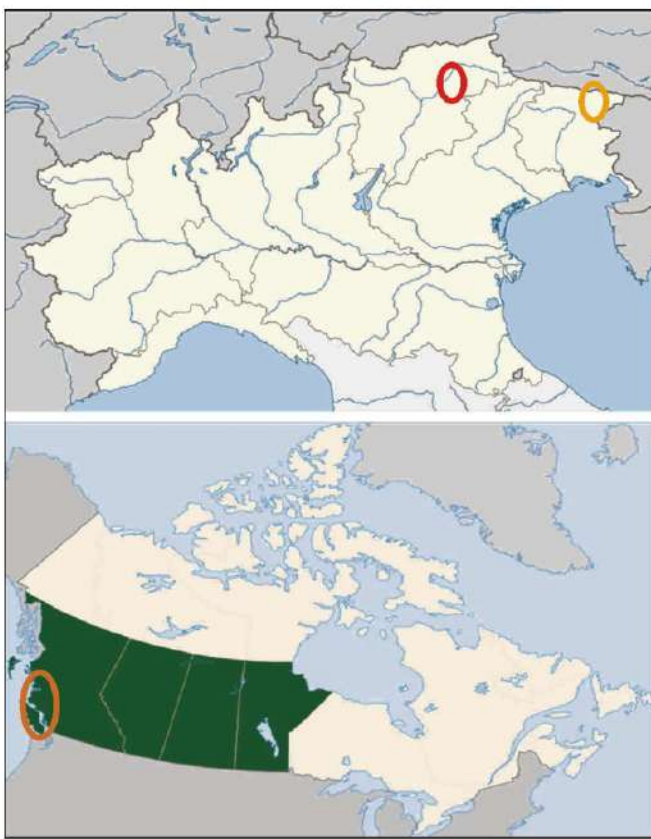


Figure 2. (Colour online) Geographic localization of different samples origin. Red circle (samples A, B and C) identifies Val di Fiemme, (Northern Italy); Yellow circle (sample D) identifies Tarvisio area (Northern East Italy); Brown circle (sample E) identifies Western Canada.

the electrons deviated from their straight path by the magnetic field of a bending magnet. The beamline is basically made up by:

- the optic hutch where the X-ray beam is prepared (energy selection, geometry definition and intensity modulation) for the specific application;
- the experimental hutches where the sample and the instrumentation are placed for investigation;
- the control room.

As illustrated by the sketch of Figure 3, the main components of the optic hutch of the beamline are the entrance vacuum slits systems, the double-crystal Si (111) monochromator and the exit air slits [40].

The monochromator works in an energy range between 83 keV and 35 keV, covering the entire angular acceptance of the beamline (ie. 7 mrad) in Bragg configuration. The beamline provides at a distance of about 23 m from the source, a monochromatic, laminar-section X-ray beam with a maximum area of about $160 \times 6 \text{ mm}^2$, measured as the FWHM of Gaussian vertical and horizontal profiles across the beam.

The described technical features of the beamline provide a geometrical resolution R of about $04 \text{ }\mu\text{m}$ at the Dod of 10 cm. The camera is water cooled too with 4008×2670 pixels and a pixel size of $45 \text{ }\mu\text{m}$. Calculated spatial resolution (PSF) is around $13 \mu\text{m}$ with a FOV of $18 \text{ mm} \times$

Table I. Samples description.

Code	Sample description
A	Spruce, high quality Origin: Val di Fiemme, Italy
B	Spruce, medium quality Origin: Val di Fiemme, Italy
C	Spruce, low quality Origin: Val di Fiemme, Italy
D	Spruce Origin: Tarvisio, Italy
E	Picea Sitchensis Origin: Canada West Coast

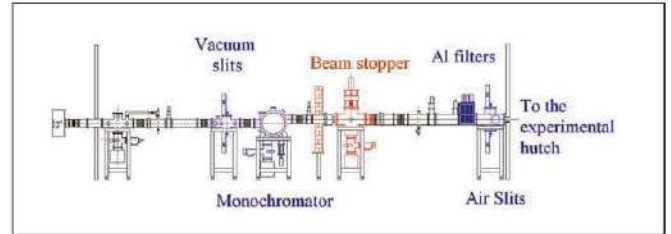


Figure 3. Sketch of the layout of the SYRMEP beamline.

12 mm. The setup for μ -CT allows performing measurements on samples having lateral dimensions slightly lower than the horizontal FOV of the CCD cameras, while different devices can be mounted on the turn-table and/or around the investigated sample for any particular in-situ measurements.

The X-ray source is furnished with a Hamamatsu L9181S tube with micrometric focal spot size ($5 \text{ }\mu\text{m}$ are assured operating at 4 W, while the maximum achievable power is 39 W), which can operate at a maximum voltage of 130 kV and a maximum current of $300 \text{ }\mu\text{A}$. The number of photons emitted per unit of time is controlled by the cathode current (usually expressed in μA). The energy of the emitted photons (expressed in eV) is controlled by the tube voltage (expressed in kV). Other significant specific parameters of the X-ray tube are summarized in the Table II.

Visual inspection of the reconstructed slices and further image processing techniques were able to reveal internal wood microstructure and important morphological features. Furthermore 3D renderings of the scanned sample helped to visualize and analyze the complex internal microstructure of vessel networks.

Once the reconstructed images (slices) and the 3D digital volume are available, an intensive and semi-automatic image processing can be applied to obtain quantitative morphological information on the wood microstructures [41]. Porosity ϕ can be evaluated as the ratio of the voids to total pixels, while the cells diameter D as well as the walls thickness w can be estimated on a statistical basis.

Different cubic pieces were cut out from the central part piano boards, with an horizontal section size of around $5 \times 5 \text{ m}^2$. No further sample preparation is necessary for

Table II. Technical characteristics of the X-ray source.

Parameter	Value/Description	Unit
X-ray Tube	Sealed Type	–
Cooling Method	Forced Air Cooling	–
Window Material	Beryllium	–
Target Material	Tungsten	–
Window Position	End-Window	–
Target Voltage	40 to 130	kV
Target Current	0 to 300	μA
Maximum Output Power	0 to 300	μA
Focal Spot Size	Small Spot Mode	8(@ 8 W),5 (@ 4 W)
	Middle Spot Mode	20(@ 16 W)
	Large Spot Mode	40(@ 39 W)
Beam Angle (Max.)	100	degree
Min. Distance Focus/Object	13	mm
Operation	Continuous	–
Focal length from outer surface of enclosure	13	Mm

tomography. A vertical thickness of around one centimetre was reconstructed slice by slice with a spatial resolution of 45 micrometres.

As stated in the introduction, the samples was analysed, graded and chosen by an outstanding piano manufacturer. A piano soundboard is quite thick compared with violin or guitar ones. So when the samples were cut out of the selected timber planks choosing the ROI, the original axis were aligned the microstructure axis. As a matter of fact, the soundboards are thick (centimetre range); thus there is a great chance to have the microstructure aligned with the right use of the board. Timber plank were selected of excellent quality so no significant variation of properties and structure could be found in any axis.

A Region of Interest (ROI) is identified as the minimum sample area, including all the necessary data related to the presented study.

To evaluate the porosity, as well as many other geometrical and morphological parameters, it is necessary to operate on a binary image (Figure 4), i.e. an image containing only 0 to represent the void phase and 1 to represent the solid phase. Once the threshold is identified, voxel is assigned to one of the two classes, according its value, if lower or higher than the threshold itself.

Quantitative analysis on reconstructed volumes and precise recognition of geometrical elements were achieved by mean of standard and custom developed software based on Matlab Imaging Toolbox 651 [42], like porosity, wall thickness and cell diameter. Not only the material density can be evaluated quantitatively, but also several purely geometrical or morphological parameters related to the cell size distribution were measured on the basis of statistical analysis. Hereafter, an example of the processing method is given (Figure 5).

22. Scanning electron microscopy investigation

The second and complementary investigation to characterize the resonance wood microstructure was the SEM analysis, necessary in order to have a clearer and brighter in-

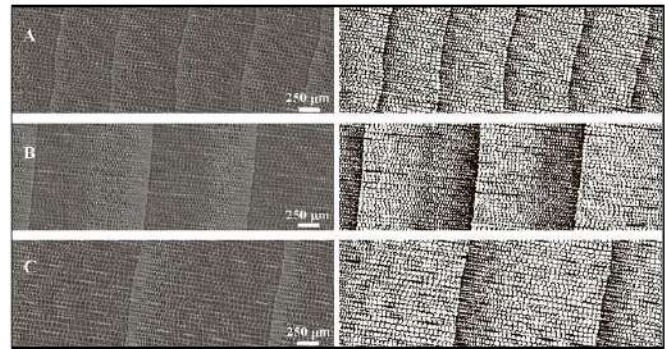


Figure 4. Original (left) and thresholded (right) wood microstructure of a Region of Interest (ROI) selected from the spruce images. High (A), medium (B) and low (C) quality samples of Spruce from Val di Fiemme, Italy.

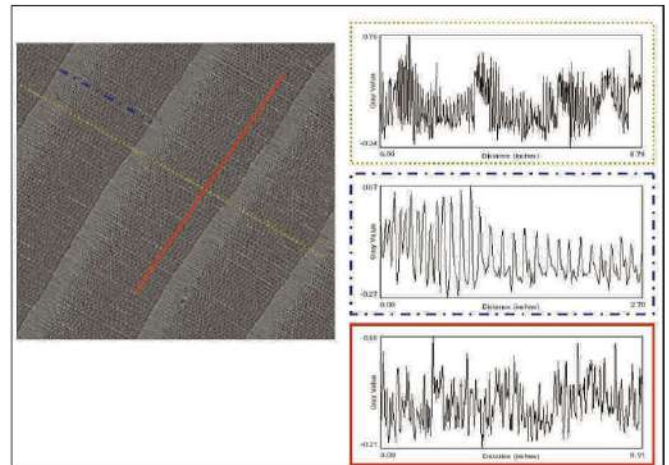


Figure 5. An example of quantitative measurements obtained from μ-CT images. Distance in μm.

sight of the microstructure itself. Using higher resolution (i.e. enlargement of 1000000 ×), it was possible to reach one nanometre of spatial resolution.

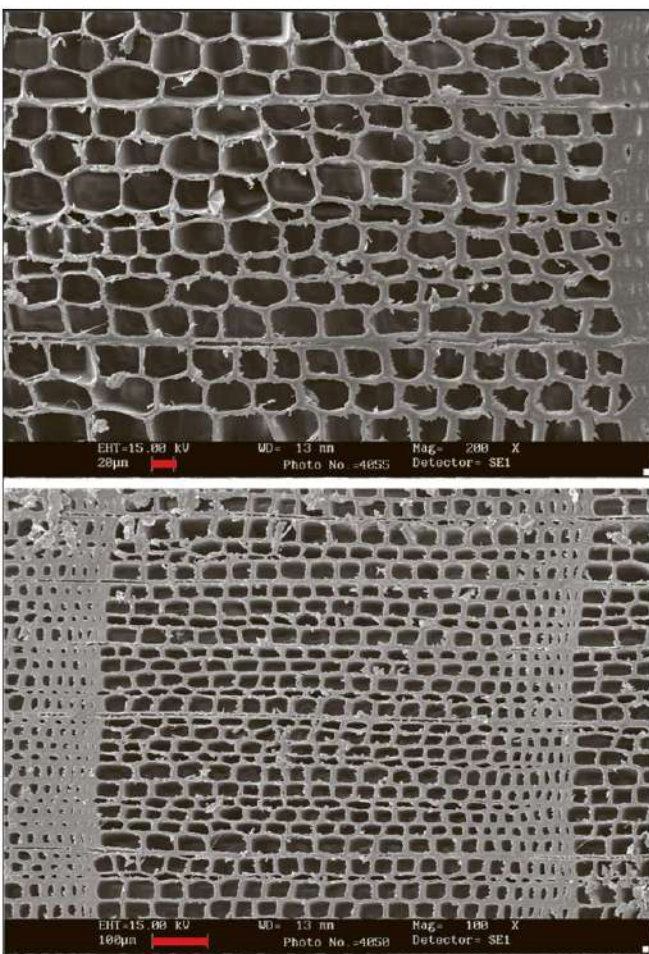


Figure 6. (Colour online) SEM pictures: early wood sample B (left); red line stands for 20 μ m. Sample A (right); red line stand for 100 μ m.

The equipment used was a Leica scanning electron microscopy Stereoscan 430i with Oxford Link X-rays microanalysis. All the specimens, as they are organic and therefore non-conductive, were previously metallized with gold.

All samples were analysed and in Figure 6 to Figure 9 some example of the inner cell microstructures are reported. The cell crush, visible for example in Figure 8, is caused by the cutting tool during samples preparation, realising waste on some of them.

23. Finite element analysis

Computer simulation was used to investigate if the microstructure of the resonance wood may influence its macro-behaviour and if the irregular geometry could determine diverse acoustic properties.

Traditionally, soundboards are modelled as thin plates or shells. In the case of the present research, the macro-behaviour is not investigated but just a very tiny and little part of the constituting material is analysed. Therefore, this little part cannot be modelled as a thin plate. Figure 10 shows an examples of the FE general results referred to the single geometry having in mind the 2D DOF applied. The aim is to determine whether the geometry of the cells

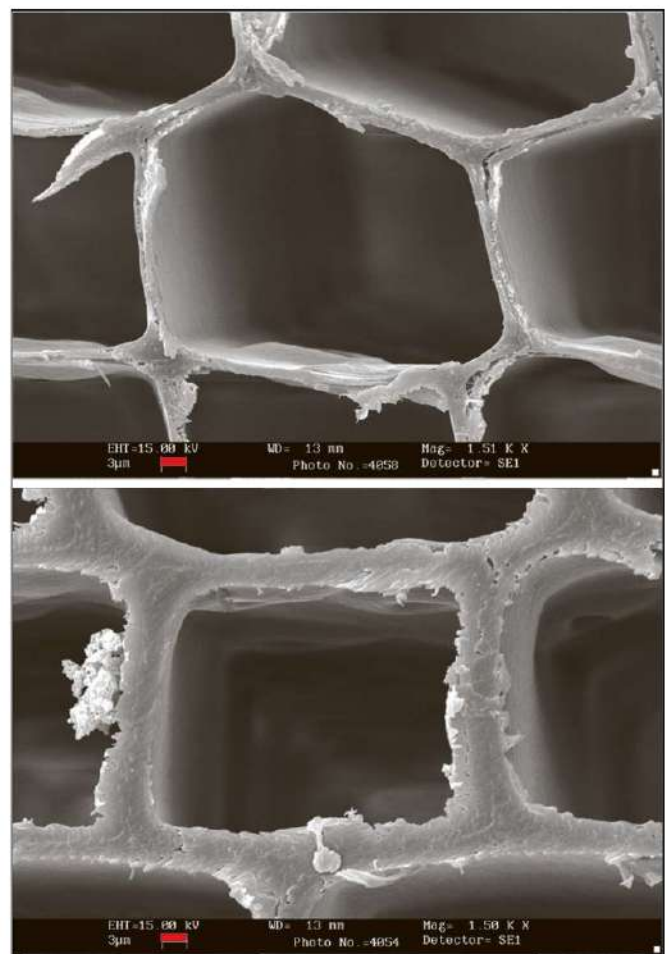


Figure 7. (Colour online) SEM pictures: early wood cell, sample B (left) and sample A (right). Both red lines stand for 3 μ m.

acts as a factor for some macro behaviour. Here the single cell contour and its influence in comparison with diverse contours is investigated.

The aim of the paper is to address the influence of single cell geometry (contour, periodicity, density, wall thickness, etc.) on the final macro behaviour. The final properties were assessed and graded by the manufacturer. Using the μ -cT on different samples cut out on diverse part of the soundboards a repeatable structure was found. So analysed ROI could be robust since the simulated and presented geometries on following figures were found in many places of the boards. The 2D wood microstructures obtained from the SEM and μ -cT analysis were simulated so as to obtain the modal behaviour versus frequency. In Figure 10, different geometries are reported; microstructures 5 and 6 were not listed since their structure contain insignificant variations compared to others.

Microstructures were drawn using μ -cT and SEM pictures in order to understand the influence of the following parameters:

- 1) cell geometry
- 2) cell density
- 3) cell shape and single cell regularity

The same cell contour highlighted on SEM and μ -cT were used in FEM simulations. Modal frequencies were

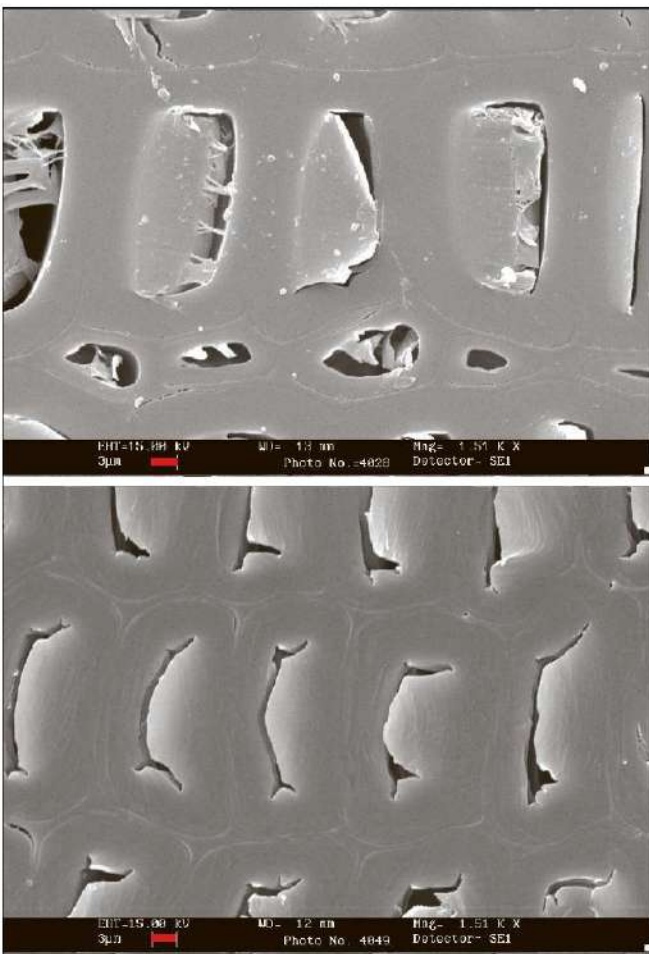


Figure 8. (Colour online) SEM pictures: late wood cell, sample B (left) and sample A (right). Both red lines stand for 3 µm.

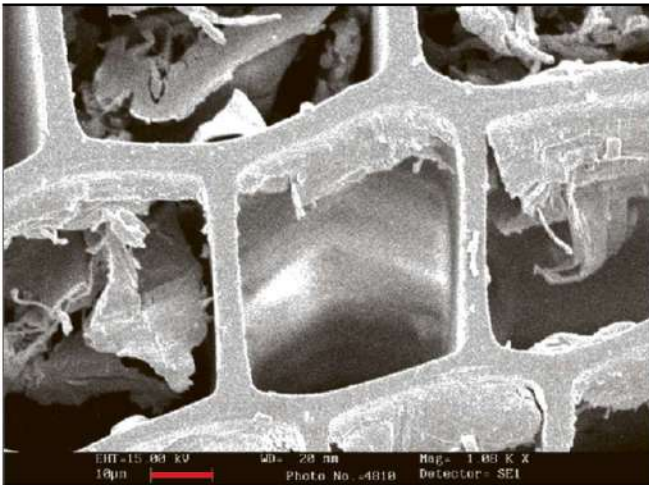


Figure 9. (Colour online) SEM pictures of early wood cell, sample D. Red line stand for 10 µm.

used to compare different microstructures acoustic behaviours. In order to understand the possible influence of the irregular single cell shape, the microstructure 3 was designed using the microstructure 2 as basis and then a regularization of the shape cell was performed.

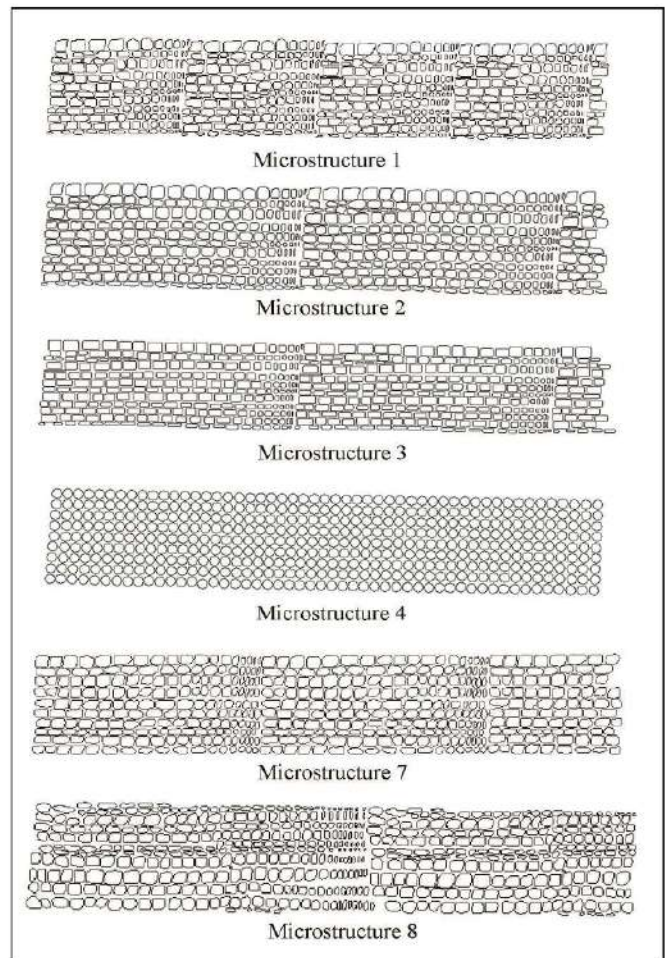


Figure 10. Micro-geometries used in finite element model.

The microstructure 4 was realized using only circular cells maintaining, the same density proportion of microstructure 2, thus permitting to comprehend the hollow regular influence. Microstructure 5 was realized lowering density by 10%. In this way the influence of this parameter was deepened.

Microstructure 6 was chosen as extreme case behaviour (continuous plate), used as comparable results with other configuration. In Table III a summary of the different simulated microstructures is reported.

Acoustic modal simulations were performed using Ansys, by means of tetragonal elements. All degrees of freedom constraints were applied on left edge of the samples, emulating a cantilever movement under acoustic impulse (piano board). In Figure 11, as an example, the first four modes of microstructure 2 are reported. The 3D model was realized with a custom-designed software package.

3. Results and discussion

The presented analyses were used to deeply investigate the resonance wood and to understand if the microstructure could influence acoustic macro-behaviour.



Figure 11. Graphical representation of the first four modes, referred to microstructure 2.

31. Microtomography analysis

Important parameters were measured using μ -CT like (i) porosity ϕ , (ii) wall thickness w and (iii) cell diameter D and reported in Table IV; in Figure 12 an example of the porosity evaluation is shown. Only the early wood outcomes are reported, because the imaging of the late wood did not appear to be precise, mainly due to sample cutting issue.

X-ray μ -CT combined with SEM techniques were used to identify a Region Of Interest on specimens in order to obtain a digital dataset (Figure 13) suitable to be investigated by imaging analysis techniques reproduced in FEM modal acoustic simulations.

32. FEM analysis

FEM simulation was conducted on 4 geometries derived from μ -CT and SEM analysis (A, C, D and E) neglecting B sample, because the medium quality did not provide relevant information. As a matter of fact, the desirable modal qualities are the ones linked to the high quality wood. The manufacturer decided the high quality and this choice in this research is voluntary taken for granted. Woodhouse [3] using Cambridge Engineering Selector and Bucur [30] demonstrate that the only modal frequencies, or Young's modulus or frequency response (objective monoparametric analyses) provide, in some way, confusing results such as (i) Ashby diagram suggests that balsa is the best resonance wood or that (ii) a cheap violin has the same performance of a Cremonese Guarneri one.

These examples demonstrate how single parameters could not completely characterize resonance wood and so the final subjective choice is of paramount importance.

In Figure 14 the original microstructures modal behaviours versus frequency are reported while in Figure 15 results from geometries variations from microstructure 2

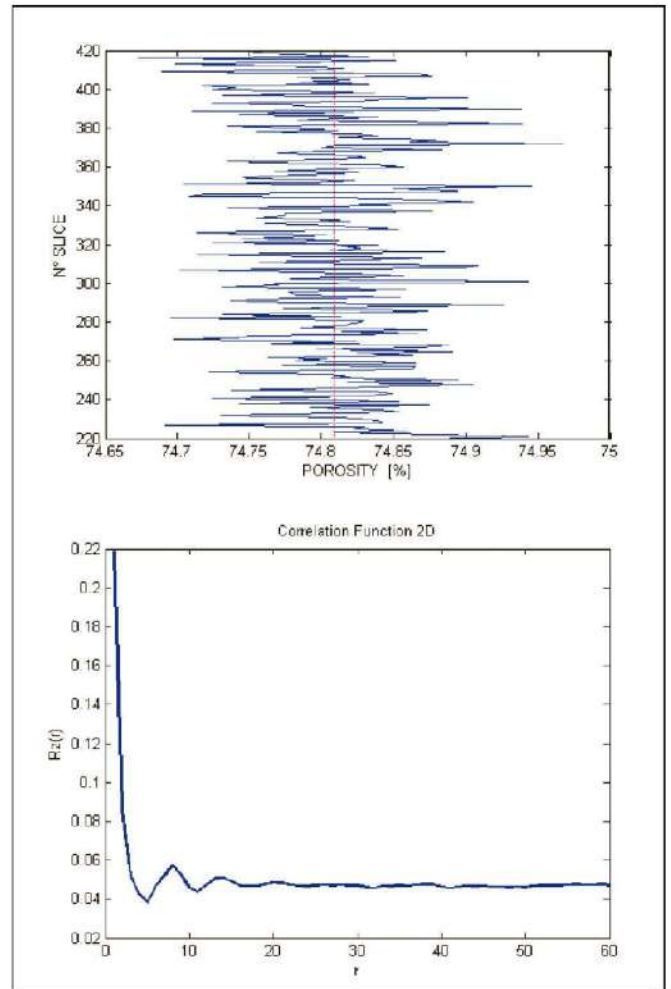


Figure 12. (Colour online) The porosity ϕ is evaluated slice by slice along the Z direction (left). Mean value is represented by the red dotted line.

are described. Analysing modal results some conclusions could be drawn:

- all microstructures from different origins provide different modal behaviours. This fact explains why musical instruments makers find different results in final products performances realized using different wood qualities;
- taking for granted that the A typology is the best one (as formerly described in section 1) and its modal behaviour is the one providing best final acoustic results, low quality Val di Fiemme Spruce (sample C) and Tarvisio one (D) show lower acoustic performances while Canada Sitka spruce (sample E) tends to be stiffer;
- from Figure 14 it is possible to see that single variation to base geometry always change modal performances.

The regularization of the cell morphology evidently acts as a stiffening since modal results rise in frequency domain and tend to the homogeneous plate performance. Small density modifications (sample 5) do not show considerable results different from sample 3 and 4 according to [30]. FEM results conclude that every cell shape modification imply a quality changing; this fact demonstrates that the

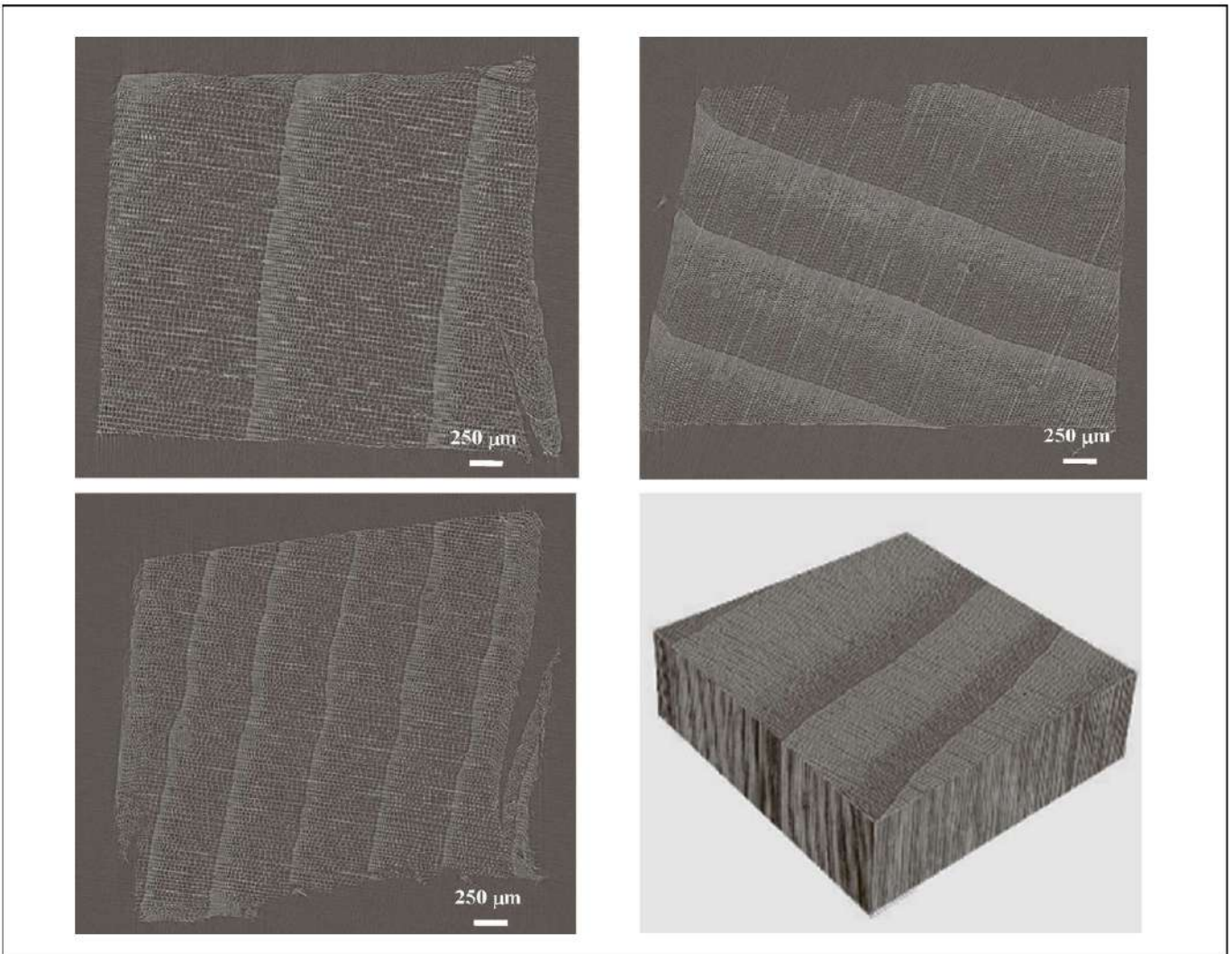


Figure 13. Reconstructed grayscale slices from Val di Fiemme wood: low quality (top left, sample C), medium quality (top right, sample B) and high quality (bottom left, sample A). Reconstructed 3D volume of sample B (bottom right).

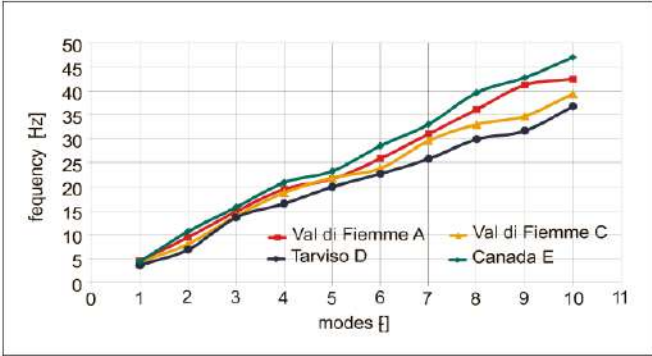


Figure 14. (Colour online) The obtained modal trend versus frequency: sample A, C, D and E.

final acoustic behaviour depends on the global microstructure and cell morphology.

Although the Tarvisio microstructure seems to be more rigid because of the larger dimension of the rings, with equally spaced and thicker cells respect to the Val di Fiemme sample A, the simulation shows a decrease of the Young's modulus; indeed, Tarvisio quality spruce (D)

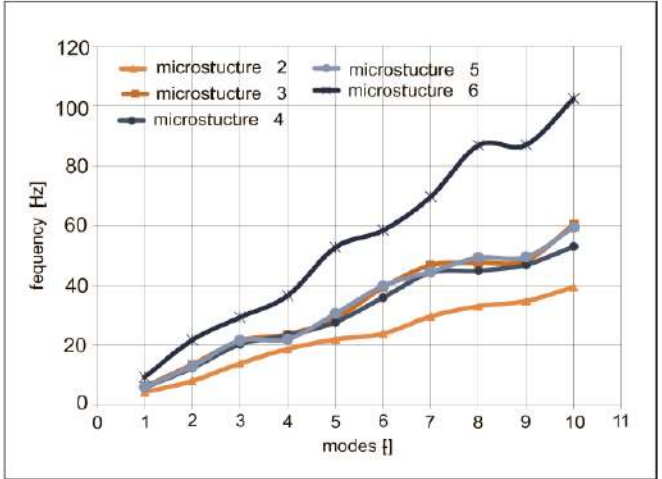


Figure 15. (Colour online) The obtained modal trend versus frequency: microstructures 2, 3, 4, 5 and 6.

clearly has a lower stiffness than the Val di Fiemme quality. On the other hand, Sitka spruce presents smaller cells wall thickness (when compared to other samples) and this

Table III. Geometrical features measured for the μ -CT reconstructed datasets. Porosity ϕ , wall thickness w and cell diameter D for early wood are reported.

	Percentile [μm]		Mean [μm]
	5%	95%	
Sample A			
ϕ	724	706	715
w	172	222	197
D	37	49	43
Sample B			
ϕ	561	612	585
w	170	235	198
D	36	51	43
Sample C			
ϕ	584	632	602
w	187	251	194
D	31	55	44
Sample D			
ϕ	683	723	703
w	178	252	214
D	32	50	41
Sample E			
ϕ	604	646	625
w	164	201	182
D	34	58	46

aspect implies that the Young's modulus across the grain decreases. These findings are in good agreement with the literature ones [30, 43] where the elastic constants were measured using wood strips methods.

33. Combination of results

FEM conclusions are in line with non-destructive tests (Figure 16). The combination of different parameters provide final acoustic results explanation. As a matter of fact, wood samples with very similar macro mechanical properties such as density, Young's modulus or shear modulus provide different acoustic final behaviour. Micro-CT analysis shows that they present different micro-geometries (cell shape and diameter, wall thickness) and could be the reason why final performances are diverse.

As an example, sample A (high quality Val di Fiemme Spruce) has the same porosity and quite the same diameter of sample D (Tarvisio Spruce), but very different wall thickness. This fact impacts on cell morphology and leads to very different final modal results. These Micro-CT results could then be matched together with SEM ones as they confirm that cell shape is the parameter influencing final performances.

Another example could be found analysing only the A, B and C samples. These all come from Val di Fiemme. Combining the three techniques, it could be understood why sample A is the best one and which parameters could influence this variation.

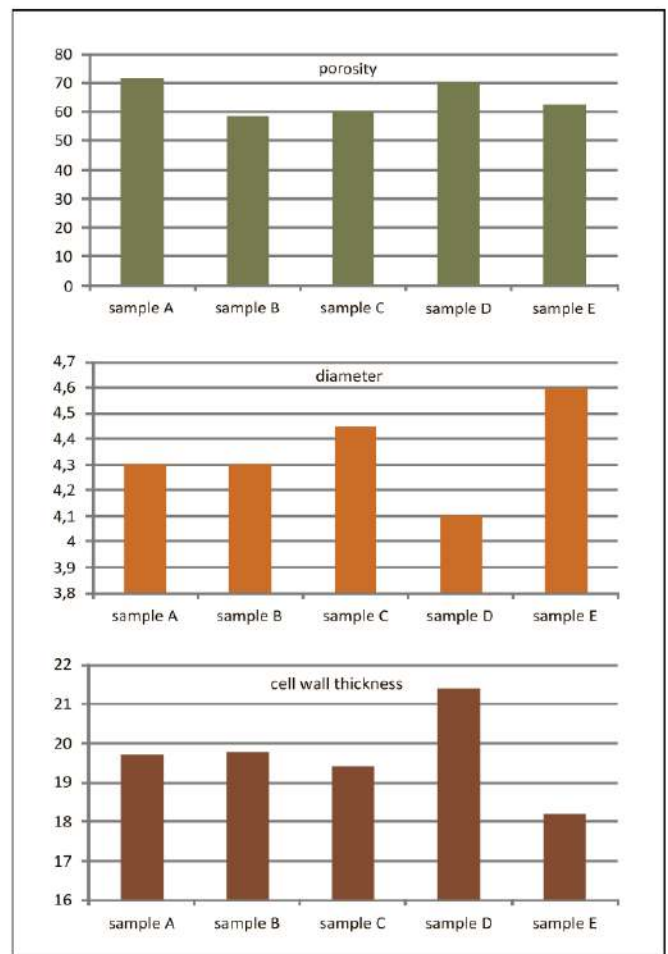


Figure 16. μ -CT results for porosity, diameter and cell wall thickness, values in μm ; results are referred to early wood.

It is evident how from micro-CT results the porosity of sample A is higher than the other two (Figure 16). The C sample highlights higher cell diameter and lower wall thickness compared to the other one. So, it could be concluded that density and cell dimensions could influence final results. FEM results show how the A sample (microstructure 1) has higher frequency response on all modes but more on the low energetic ones. This behaviour highlights the influence of the cell shape on single microstructure and links the porosity and cell wall thickness results obtained from micro-CT. FEM results demonstrated that the variation on the cell geometry provides very different acoustic behaviour (Figure 15), highlighting that small geometry variations could lead to a very different acoustic behaviour.

Actually, in the same figure it is demonstrated how the variation of the density of 10% could not lead to significant acoustic differences, but a small deviation on cells shape (microstructure 2 vs. microstructure 3 – ref. Figure 10) implies sensible acoustic results modification. These results demonstrate how the two technologies provide similar results using diverse points of view and the combined used demonstrate finally that final performances could not be associated just to macro characteristics like density or

Young's Modulus, but that they are influenced also by cells geometry and cells geometrical parameters.

Only using combined techniques it could be possible to understand why for example Tarvisio spruce is not considerable as good as high quality Val di Fiemme one. This is demonstrated by the fact that it has a comparable porosity to sample A but cell diameter and cell wall thickness are very different (Figure 16). Using FEM modal technique it could be reported that Sample D has the lowest frequency response and thus radiation effects could not be as effective as Sample A. In this case too, the combination of the two technologies explain final behaviours.

Sample E represents the opposite results compared to Tarvisio sample in terms of cells diameter and wall thickness. This provides a very different acoustic behaviour (Figure 14), because the Canadian Spruce seems radiate too much easily the acoustic impulse. This, from a scientific point of view, could provide a good point, but from a macroscale point of view it is not considered a good performance. As previously said, Sample A behaviour is to be considered the best one. In this view, Sample E "passes the line".

4. Conclusions

In this paper a scientific method based on innovative techniques was described and used in order to assess different quality of resonance wood.

Several microstructures were tested and compared with X-ray microtomography and scanning electron microscopy coupled with finite element method. The results show different trend of the analysed micro-geometries motivating the choice of best wood quality usable to realize musical instruments. The presented results aim to demonstrate the clear dependence of the macro-acoustical characteristics on the global microstructure of the resonance woods.

FEM results clearly show that different microstructures morphologies influences final acoustic macro-behaviour. The simulated results are in line by microtomography outcomes on cell geometries, showing how the whole set of variation on wall thickness, porosity and cell diameters influence final performances.

Results show different trends of woods varieties and therefore different acoustic macro-behaviours and then this method could be used to characterize resonance wood.

Future works would be systematic structure-property correlations and a better fundamental understanding of Spruce wood identifying key parameters (eg. cell size, cell geometry -eg. hexagonal versus rectangular-, cell wall thickness) determining the mechanical and acoustical properties of the wood.

Acknowledgement

This research was funded project D4, FSE, Friuli Venezia Giulia Region promoted by Italian Ministry of Work.

The Authors would like to thank Fazioli Pianoforti for the information and wood samples and the two anonymous reviewers for their precious help and valuable comments.

Marco Caniato collected, elaborated and described all the reported data. Stefano Favretto performed Micro-ct analysis. Marco Caniato and Federica Bettarello performed acoustics test. Marco Caniato performed and analyzed acoustic numerical simulations. Chiara Schmid overviewed the research. Marco Caniato wrote the paper.

References

- [1] Y. Yang, Z. Liu, Y. Liu: Prediction of lute acoustic quality based on soundboard vibration performance using multiple choice model. *J. For. Res.* **28** (2017) 855–861.
- [2] C. Buksnowitz: Resonance wood [Piceaabies (L.) Karst.] Evaluation and prediction of violin makers' quality-grading. *J Acoust Soc Am* **121** (2007) 2384–2395.
- [3] J. Woodhouse: The acoustics of the violin: a review. *Reports on Progress in Physics*, Volume 77, Number 11, 2014.
- [4] P. Horcin, V. Gubriansky: Properties of wood in musical instruments making. *Proc. Forum Acusticum*, Budapest, 28/8-2/9 2005.
- [5] J. Berthaut, M. N. Ichchou, L. Jézéquel: Piano soundboard: structural behavior, numerical and experimental study in the modal range. *Appl. Acoust.* **64** (2003) 1113–1136.
- [6] H. Suzuki, I. Nakamura: Acoustics of pianos. *Appl. Acoust.* **30** (1990) 147–205.
- [7] C. M. Hutchins: Measurable characteristics of violin-family instruments in relation to the sound of a high-quality violin. *MRS Bulletin*, March 1995, pp. 29-31.
- [8] I. Brémaud: Acoustical properties of wood in string instruments soundboards and tuned idiophones: biological and cultural diversity. *J. Acoust. Soc. Am.* **131** (2012) 807–818.
- [9] I. Brémaud: What do we know on "resonance wood" properties? Selective review and ongoing research. *Societe Francaise d'Acoustique. Acoustics 2012*, Apr 2012, Nantes, France, 2012.
- [10] J. C. Schelleng: The violin as a circuit. *Journal of the Acoustical Society of America* **35** (1963) 326.
- [11] C. Y. Barlow: Materials selection for musical instruments. *Proceedings - Institute of Acoustics*, 1997, 69–78. *Musical acoustics: ISMA'97*.
- [12] J. H. Fromm, et al: Xylem water content and wood density in spruce and oak trees detected by high-resolution computed tomography. *Plant Physiol.* **127** (2001) 416–425.
- [13] L. Brancheriau, H. Baillères, P. Détienne, R. Kronland, B. Metzger: Classifying xylophone bar materials by perceptual, signal processing and wood anatomy analysis. *Ann For Sci* **63** (2006) 73–81.
- [14] J. A. M. Rojas, J. Alpuente, D. Postigo, I. M. Rojas, S. Vignote: Wood species identification using stress-wave analysis in the audible range. *Applied Acoustics* **72** (2011) 934–942.
- [15] V. Bucur, P. Lancelleur, B. Roge: Acoustic properties of wood in tridimensional representation of slowness surfaces. *Ultrasonics* **40** (2002) 537–541.
- [16] F. C. Beall: Overview of the use of ultrasonic technologies in research on wood properties. *Wood Sci. Technol.* **36** (2002) 197–212.
- [17] R. Corradi, S. Miccoli, G. Squicciarini, P. Fazioli: Modal analysis of a grand piano soundboard at successive manufacturing stages. *Applied Acoustics* **125** (2017) 113–127.
- [18] K. Ege, X. Boutillon, M. Rébillat: Vibroacoustics of the piano soundboard: (non)linearity and modal properties in the

- low- and mid-frequency ranges. *J Sound Vib* **332** (2013) 1288–1305.
- [19] P. Mania, E. Fabisiak, E. Skrodzka: Investigation of modal behaviour of resonance spruce wood samples (Spruce I.). *Archives of Acoustics* **42** (2017) 23–28.
- [20] G. Squicciarini, P. Miranda Valiente, D. J. Thompson: Sound power and vibration levels for two different piano soundboards. *J. Physics: Conf. Series* **744** (2016) 012091.
- [21] M. Caniato, F. Bettarello, P. Fausti, L. Marsich, A. Ferluga, C. Schmid: Impact sound of timber floors in sustainable buildings. *Build. Environ.* **120** (2017) 110–122.
- [22] M. Caniato, F. Bettarello, A. Ferluga, L. Marsich, C. Schmid, P. Fausti: Acoustic of lightweight timber buildings: a review. *Renew. Sust. En. Rev.* **80C** (2017) 585–596.
- [23] A. Mamou-Mani, S. Le Moyne, F. Ollivier, C. B esnainou, J. Frelat: Prestress effects on the eigenfrequencies of the soundboards: experimental results on a simplified string instrument. *J Acoust Soc Am* **131** (2012) 872–877.
- [24] J. Bretos, C. Santamaría, J. Alonso Moral: Finite element analysis and experimental measurements of natural eigenmodes and random responses of wooden bars used in musical instruments. *Applied Acoustics* **56** (1999) 141–156.
- [25] X. Boutillon, K. Ege: Vibroacoustics of the piano soundboard: Reduced models, mobility synthesis, and acoustical radiation regime. *J. Sound. Vib.* **332** (2013) 4261–4279.
- [26] U. G. K. Wegst: Wood for sound. *American Journal of Botany* **93** (2006) 1439–1448.
- [27] W. Moliński, E. Roszyk, J. Puszyk: i: Variation in mechanical properties within individual annual rings of the resonance spruce wood [Spruce (L.) Karst]. *Drvna industrija* **65** (2014) 215–223.
- [28] M. Spycher, F. W. M. R. S chwarze, R. Steiger: Assessment of resonance wood quality by comparing its physical and histological properties. *Wood Sci. Technol.* **42** (2008) 325–342.
- [29] A. R. Proto, G. Macrí, V. Bernardini, D. Russo, G. Zimbalatti: Acoustic evaluation of wood quality with a non-destructive method in standing trees: a first survey in Italy. *IForest* **10** (2017) 700–706.
- [30] V. Bucur: *Acoustics of wood*. Springer Verlag, Berlin Heidelberg, 2006.
- [31] F. G. O. Pearson, C. Webster: *Timber used in the musical instrument industry*. Forest Products Laboratory, Ministry of Technology, London, 1967.
- [32] D. Holz, J. Schmidt: Untersuchungen an Resonanzholz. IV. Mitteilung: Über den Zusammenhang zwischen statisch und dynamisch bestimmten Elastizitätsmodulen und die Beziehung zur Rohdichte bei Fichtenholz. *Holztechnologie* **9** (1968) 225–229.
- [33] T. Ono, A. Kataoka: The frequency dependence of the dynamic modulus and internal friction of wood used for the soundboards of musical instruments. Part I: Effect of rotary inertia and shear on the flexural vibration of free-free beams. *Mokuzai Gakkaishi* **25** (1979) 461–468. Part II: The dependence of the Young's modulus and internal friction on frequency, 535–542.
- [34] M. Caniato, S. Favretto, E. Lucchini: Comparison between different resonance woods by a new scientific method. 19th International Congress on Acoustics, Madrid, 2-7 september 2007.
- [35] M. Caniato, S. Favretto, E. Lucchini: A new approach for the characterization of the resonance wood. 19th International Congress on Acoustics, Madrid, 2-7 september 2007.
- [36] L. L. Gibson, M. F. Ashby: *Cellular solids*. Cambridge University Press, 2014.
- [37] E. Kahle, Woodhouse: The influence of cell geometry on the elasticity of softwood. *J Mater Sci* **29** (1994) 1250.
- [38] B. Illman, B. Dowd: High resolution microtomography for density and spatial information about wood structures. SPIE's 44th Annual Meeting and Exhibition: The International Symposium on Optical Science, Engineering and Instrumentation, Denver, Colorado, USA, 18-23 July 1999.
- [39] K. Steppe, et al: Use of X-ray computed microtomography for non-invasive determination of wood anatomical characteristics. *Journal of Structural Biology* **148** (2004) 11–21.
- [40] F. Arfelli, G. Barbiellini, P. Bregant, F. Calligaris, G. Cantatore, E. Castelli, L. Dalla Palma, F. de Guarrini, R. Giacomich, R. Longo, P. Poropat, R. Rosei, M. Sessa, F. Stacul, M. Tonutti, F. Tomasini, G. Tromba, A. Vacchi, R. Vidimari, F. Zanini, C. Z uiani: Synchrotron radiation for medical physics. A comparison between digital and conventional screen-film systems. *Phys. Med.* **9** (1993) 188–191.
- [41] J. Serra: *Image analysis and mathematical morphology*. Academic Press, London, 1982.
- [42] W. K. Pratt: *Digital image processing*. J. Wiley and Sons, New York, 1978.
- [43] D. Haines: On musical instrument wood. *Catgut Acoust Soc Newsl* **1** (1979) 23–32.